Atmos. Chem. Phys. Discuss., https://doi.org/10.5194/acp-2018-334
Manuscript under review for journal Atmos. Chem. Phys.
Discussion started: 14 May 2018

Atmospheric Chemistry and Physics Discussions

Atmospheric $\Delta^{17}O(NO_3^-)$ reveals nocturnal chemistry dominates nitrate production in Beijing haze

Pengzhen He[1], Zhouqing Xie[1,2,3]*, Xiyuan Chi[1], Xiawei Yu[1], Shidong Fan[1], Hui Kang[1], Cheng Liu[1,2,3], Haicong Zhan[1]

[1]Anhui Province Key Laboratory of Polar Environment and Global Change, School of Earth and Space Sciences, University of Science and Technology of China, Hefei, Anhui 230026, China.

[2]Key Lab of Environmental Optics and Technology, Anhui Institute of Optics and Fine Mechanics, Chinese Academy of Sciences, Hefei, Anhui 230031, China.

[3]Center for Excellence in Urban Atmospheric Environment, Institute of Urban Environment, Chinese Academy of Sciences, Xiamen, Fujian 361021, China.

**Corresponding to*: Zhouqing Xie (zqxie@ustc.edu.cn)

Abstract. The rapid mass increase of atmospheric nitrate is a critical driving force for the occurrence of fine-particle pollution (referred to as haze hereafter) in Beijing. However, the exact mechanisms for this rapid increase of nitrate mass has been not well constrained from field observations. Here we present the first observations of the oxygen-17 excess of atmospheric nitrate ($\Delta^{17}O(NO_3^-)$) collected in Beijing haze to reveal the relative importance of different nitrate formation pathways, and we also present the simultaneously observed $\delta^{15}N(NO_3^-)$. During our sampling period, 12h-averaged mass concentrations of $PM_{2.5}$ varied from 16 to 323 μg m^{-3} with a mean of (141±88 (1σ)) μg m^{-3}, with nitrate ranging from 0.3 to 106.7 μg m^{-3}. The observed $\Delta^{17}O(NO_3^-)$ ranged from 27.5 ‰ to 33.9 ‰ with a mean of (30.6±1.8) ‰ while $\delta^{15}N(NO_3^-)$ ranged from –2.5 ‰ to 19.2 ‰ with a mean of (7.4±6.8) ‰. $\Delta^{17}O(NO_3^-)$-constrained calculations suggest nocturnal pathways (N_2O_5 + H_2O/Cl^- and NO_3 + HC) dominated nitrate production during polluted days ($PM_{2.5} \geq 75$ μg m^{-3}) with the mean possible fraction of 56 – 97 %. For $\delta^{15}N(NO_3^-)$, we found that a combined effect of variability in NO_X sources and isotopic exchange between NO and NO_2 is likely to be most responsible for its variations. Our results illustrate the potentiality of isotope in tracing NO_X sources and nitrate formation pathways, future modelling work with the constraint of isotope data reported here may further improve our understanding of nitrogen cycle during haze.

1 Introduction

Severe and frequent haze pollution has become a crucial threat for the air quality in megacity Beijing and the North China Plain in recent years. The high concentrations of $PM_{2.5}$ (particulate matter with an aerodynamic diameter equal or less than 2.5 μm) during severe haze, of which the hourly average can reach 1000 μg m^{-3} (Zheng et al., 2015a), is harmful

Atmos. Chem. Phys. Discuss., https://doi.org/10.5194/acp-2018-334
Manuscript under review for journal Atmos. Chem. Phys.
Discussion started: 14 May 2018

Atmospheric Chemistry and Physics Discussions

to the public health by contributing to cardiovascular morbidity and mortality (Cheng et al., 2013; Brook et al., 2010). Nitrate is an important component of $PM_{2.5}$, accounting for 1–45 % of $PM_{2.5}$ mass in Beijing and North China Plain (Wen et al., 2015; Zheng et al., 2015a; Zheng et al., 2015b). The main formation pathways of atmospheric nitrate in urban area are summarized in Fig. 1, which includes: (i) NO_2 oxidation by OH radical in the gas-phase, (ii) heterogeneous uptake of NO_2 on wet aerosols, (iii) NO_3 radical reacting with hydrocarbon (HC), and (iv) heterogeneous uptake of N_2O_5 on wet aerosols and chlorine-containing aerosols. Since OH radical is mainly present in the daytime while NO_3 radical and N_2O_5 are mainly present in the nocturnal atmosphere (Brown and Stutz, 2012), NO_2 + OH is usually referred as the daytime nitrate formation pathway while N_2O_5 + H_2O/Cl^- and NO_3 + HC are referred as nocturnal formation pathways (Vicars et al., 2013; Sofen et al., 2014). During haze in Beijing, the mixing ratio of daytime OH is modelled to be low (Zheng et al., 2015b; Rao et al., 2016) while relatively high mixing ratio of nocturnal N_2O_5 is observed in several studies (Wang et al., 2017a; Li et al., 2018; Wang et al., 2017b), therefore, nocturnal pathways are suggested to be most responsible for the high concentrations of atmospheric nitrate during haze (Su et al., 2017; Pathak et al., 2009; Pathak et al., 2011). In addition, the high $PM_{2.5}$ concentration and relative humidity during haze in Beijing favors heterogeneous reactions, which renders NO_2 + H_2O being a potentially significant pathway for nitrate production (Wang et al., 2017d; Tong et al., 2015; Zheng et al., 2015a).

Nitrogen isotopic composition of nitrate ($\delta^{15}N(NO_3^-)$, wherein $\delta^{15}N = (R_{sample}/R_{reference} - 1)$ with R representing isotope ratios of $^{15}N/^{14}N$ in the sample and the reference atmospheric N_2) is useful in tracing source of its precursor NO_X (Xiao et al., 2015; Beyn et al., 2014; Fang et al., 2011; Hastings et al., 2013). Anthropogenic sources of NO_X such as coal combustion are generally enriched in $\delta^{15}N$ while natural NO_X sources such as soil emissions or lighting typically have negative or zero $\delta^{15}N$ signature (Hoering, 1957; Yu and Elliott, 2017; Felix et al., 2012). Therefore highly positive values of observed $\delta^{15}N(NO_3^-)$ can be considered as an indicator of anthropogenic combustion (Elliott et al., 2009; Fang et al., 2011), although this judgment may be influenced by isotopic exchange between NO and NO_2 (Freyer et al., 1993; Walters et al., 2016). The oxygen-17 excess ($\Delta^{17}O$) of nitrate, defined as $\Delta^{17}O = \delta^{17}O - 0.52\delta^{18}O$, wherein $\delta^{X}O = (R_{sample}/R_{reference} - 1)$ with R representing isotope ratios of $^{X}O/^{16}O$ in the sample and the reference Vienna Standard Mean Ocean Water and X = 17 or 18, is particularly useful in reflecting nitrate formation pathways (Michalski et al., 2003). Atmospheric nitrate from nocturnal reaction pathways has higher $\Delta^{17}O$ than that from daytime OH oxidation at given $\Delta^{17}O(NO_2)$ (Table 1). And once formed, atmospheric $\Delta^{17}O(NO_3^-)$ cannot be altered by mass-dependent processes such as deposition during transport (Brenninkmeijer et al., 2003). Previous studies have shown the utility of atmospheric $\Delta^{17}O(NO_3^-)$ in quantifying the relative importance of various nitrate formation pathways (Alexander et al., 2009; Michalski et al., 2003; Patris et al., 2007; Savarino et al., 2013; Vicars et al., 2013). For example, $\Delta^{17}O(NO_3^-)$-constrained box modeling work of Michalski et al. (2003) suggests that more than 90 % of atmospheric nitrate is from nocturnal N_2O_5 + H_2O pathway in winter La Jolla, California, which is reflected by the highest $\Delta^{17}O(NO_3^-)$ values being observed in winter. In another study, Alexander et al. (2009) use observed $\Delta^{17}O(NO_3^-)$

to constrain 3D model and found that daytime NO_2 + OH pathway dominates global tropospheric nitrate production with an annual mean contribution of 76 %.

Until now, however, field observations of atmospheric $\Delta^{17}O(NO_3^-)$ have not been conducted in north China to constrain the relative importance of different nitrate formation pathways during haze. In this work, we present the first observations of atmospheric $\Delta^{17}O(NO_3^-)$ during Beijing haze from October 2014 to January 2015, and use this observation to examine the importance of nocturnal formation pathways. We also present the signature of simultaneously observed $\delta^{15}N(NO_3^-)$ and discuss its potential influencing factors.

2 Materials and Methods

2.1 Sampling and atmospheric observations

$PM_{2.5}$ filter samples were collated at a flow rate of 1.05 m^3 min^{-1} by a high volume air sampler (model TH-1000C II, Tianhong Instruments Co., Ltd, China). The filter is quartz microfiber filter (Whatman Inc., UK), pre-combusted at 450 °C for 4 h before sampling. Our sampling period lasted from October 2014 to January 2015 with the collection interval being 12 h (08:00 – 20:00 LT or 20:00 – 08:00 LT) for each sample. Blank control samples were also collected. The blank was sampled identically to the real sample except that the collection interval is 1 min. Due to that gaseous HNO_3 is likely to adsorb onto particulate matter already trapped by the filter material (Vicars et al., 2013), the nitrate species collect here is likely to include both particulate nitrate and gaseous HNO_3, which is referred to as atmospheric nitrate in previous studies (Vicars et al., 2013; Morin et al., 2009; Michalski et al., 2003) and in this study. The sample site is at the campus of University of the Chinese Academy of Sciences (40.41 ° N, 116.68 ° E, ~20 m high) in suburban Beijing, about 60 km northeast of downtown (Fig. 2), which is a supersite set by HOPE-J^3A (Haze Observation Project Especially for Jing-Jin-Ji Area) with various observations being reported (Zhang et al., 2017; Xu et al., 2016; Chen et al., 2015; Tong et al., 2015; He et al., 2017). Hourly concentrations of surface $PM_{2.5}$, CO, SO_2, NO_2 and O_3 were observed at Huairou station (40.33 ° N, 116.63 ° E) by Beijing Municipal Environmental Monitoring Center, about 10 km to our sampling site. Meteorological data including relative humidity (RH) and air temperature (*T*) were measured by an automatic weather station (model MetPak, Gill Instruments Limited, UK). Time used in the present study is local time (LT = UTC + 8).

2.2 Measurements of ions and isotopic ratios

Ion concentrations of NO_3^- and Cl^- were measured in Anhui Province Key Laboratory of Polar Environment and Global Change in the University of Science and Technology of China. A detailed description of this method can be found in the

literature (Ye et al., 2015). Briefly, ions in the $PM_{2.5}$ filter sample were extracted with Millipore water (≥ 18 MΩ) and insoluble substances in the extract were filtered. Then the ion concentrations were analyzed by an ion chromatograph system (model Dionex ICS-2100, Thermo Fisher Scientific Inc., USA). The measured ion concentrations of blank samples were subtracted when determine the ion concentrations of real samples. Typical analytical precision by our method is better than 10 % relative standard deviation (RSD) (Chen et al., 2016).

$\delta^{15}N(NO_3^-)$ and $\Delta^{17}O(NO_3^-)$ were measured with a bacterial denitrifier method (Kaiser et al., 2007) in IsoLab at the University of Washington, USA. Briefly, ions in the filter sample were extracted with Millipore water (≥ 18 MΩ) and the insoluble substances were filtered. NO_3^- in each sample was converted to N_2O by the denitrifying bacteria, Pseudomonas aureofaciens. Then N_2 and O_2, which were decomposed from N_2O in a gold tube at 800 ° C, were separated by a gas chromatograph. The isotopic ratios of each gas were then measured by a Finnigan Delta-Plus Advantage isotope ratio mass spectrometer. Masses of 28 and 29 from N_2 were measured to determine $\delta^{15}N$. Masses of 32, 33 and 34 from O_2 were measured to determine $\delta^{17}O$ and $\delta^{18}O$ and $\Delta^{17}O$ was then calculated. We use international nitrate reference materials, USGS34, USGS35 and IAEANO_3, for data calibration. The uncertainty (1σ) of $\delta^{15}N$ and $\Delta^{17}O$ measurements in our method is 0.4 ‰ and 0.2 ‰, respectively, based on replicate analysis of the international reference materials. All the samples including blank samples were measured in triplicate to quantify the uncertainty in each sample. The blank was subtracted for each sample by using an isotopic mass balance on the basis of isotopic ratios and concentrations of the blank. To minimize the blank effect, samples with blank concentrations > 10 % of their concentrations were not analyzed for isotopic ratios. This ruled out 3 of the total 34 samples, all of which are in non-polluted days (NPD, $PM_{2.5}$ < 75 μg m^{-3}). Totally, isotopic compositions of 7 samples in NPD and 24 samples in polluted days (PD, $PM_{2.5}$ ≥ 75 μg m^{-3}) are reported here.

2.3 Estimate of different nitrate formation pathways based on $\Delta^{17}O(NO_3^-)$

The observed $\Delta^{17}O(NO_3^-)$ is determined by the relative importance of different nitrate formation pathways and the relative importance of O_3 oxidation in NO_X cycling as shown in Eq. (1):

$$\Delta^{17}O(NO_3^-) = \Delta^{17}O_{R6} \times f_{R6} + \Delta^{17}O_{R7} \times f_{R7} + \Delta^{17}O_{R8} \times f_{R8} + \Delta^{17}O_{R9} \times f_{R9} + \Delta^{17}O_{R10} \times f_{R10} \quad (1)$$

Where $\Delta^{17}O_{R6}$, $\Delta^{17}O_{R7}$, $\Delta^{17}O_{R8}$, $\Delta^{17}O_{R9}$ and $\Delta^{17}O_{R10}$ is respectively $\Delta^{17}O(NO_3^-)$ resulting from NO_2 + OH, NO_2 + H_2O, NO_3 + HC, N_2O_5 + H_2O and N_2O_5 + Cl^- pathway. f_{R6}, f_{R7}, f_{R8}, f_{R9} and f_{R10} is respectively corresponding fractional contribution of above pathways to nitrate production. By using the assumptions in Table 1 and the definition $f_{R6} + f_{R7} + f_{R8} + f_{R9} + f_{R10} = 1$, Eq. (1) is further expressed as:

$$\Delta^{17}O(NO_3^-)/‰ = 24.85\alpha f_{R6} + 24.85\alpha f_{R7} + (24.85\alpha + 13.66) \times f_{R8} + (24.85\alpha + 6.83) \times f_{R9} + (24.85\alpha + 13.66) \times f_{R10} = 24.85\alpha + 13.66 \times (f_{R8} + f_{R10}) + 6.83 f_{R9} \quad (2)$$

Where α is the proportion of O_3 oxidation in NO_X cycling, calculated by Eq. (3):

$$\alpha = \frac{k_{R1}[NO][O_3]}{k_{R1}[NO][O_3]+k_{R2a}[NO][HO_2]+k_{R2b}[NO][RO_2]} \quad (3)$$

In Eq. (3), k_{R1}, k_{R2a} and k_{R2b} is respectively the reaction rate constant listed in Table 2. To evaluate α, we estimated HO_2 mixing ratios on the basis of empirical formulas between HO_2 and O_3 mixing ratios derived from observations in winter (Kanaya et al., 2007), that's: $[HO_2]/(\text{pmol mol}^{-1}) = \exp(5.7747\times10^{-2}\times[O_3]/(\text{nmol mol}^{-1}) - 1.7227)$ during the day time and $[HO_2]/(\text{pmol mol}^{-1}) = \exp(7.7234\times10^{-2}\times[O_3]/(\text{nmol mol}^{-1}) - 1.6363)$ at night. Then RO_2 mixing ratio was calculated as 70 % of HO_2 mixing ratios based on previous studies (Liu et al., 2012; Elshorbany et al., 2012; Mihelcic et al., 2003). As NO mixing ratio was not observed in our study, we estimated NO mixing ratios following the empirical formulas between NO_X and CO mixing ratios derived from observations in winter Beijing (Lin et al., 2011), that's: $[NO]/(\text{nmol mol}^{-1}) = ([CO]/(\text{nmol mol}^{-1}) - 196)/27.3 - [NO_2]/(\text{nmol mol}^{-1})$ during daytime and $[NO]/(\text{nmol mol}^{-1}) = ([CO]/(\text{nmol mol}^{-1}) - 105)/30.9 - [NO_2]/(\text{nmol mol}^{-1})$ at night.

By using Eq. (2), the relative importance of nocturnal formation pathways ($f_{R8} + f_{R9} + f_{R10}$) can be written as Eq. (4):

$$f_{R8} + f_{R9} + f_{R10} = \frac{f_{R9}}{2} + \frac{\Delta^{17}O(NO_3^-)}{13.66‰} - 1.82\alpha \quad (4)$$

Eq. (4) suggests that the relative importance of nocturnal pathways is solely a function of the assumption of f_{R9} at given $\Delta^{17}O(NO_3^-)$ and α. Since f_{R9}, $f_{R8} + f_{R10}$ and $f_{R8} + f_{R9} + f_{R10}$ should be in the range of 0 – 1 at the same time, f_{R9} is further limited to meet Eq. (5):

$$f_{R9}\begin{cases} > 0 \\ < \min(1, \frac{\Delta^{17}O(NO_3^-)}{6.83‰} - 3.64\alpha, 2 + 3.64\alpha - \frac{\Delta^{17}O(NO_3^-)}{6.83‰}) \end{cases} \quad (5)$$

We estimated the relative importance of nocturnal pathways ($f_{R8} + f_{R9} + f_{R10}$) by using concentration-weighted $\Delta^{17}O(NO_3^-)$ observations and production rate weighted α in PD of each haze event rather than each sample due to the lifetime of atmospheric nitrate is typically on the order of days (Vicars et al., 2013), larger than our sampling collection interval.

2.4 Simulation of surface N_2O_5 and NO_3 radical

We use the Master Chemical Mechanism (MCM, version 3.3, http://mcm.leeds.ac.uk/) to simulate the mixing ratios of surface N_2O_5 and NO_3 radical during our sampling period. The input for this modeling work includes: (i) 1 h-averaged mixing ratios of observed surface CO, NO_2, SO_2 and O_3 and estimated NO (see Sect. 2.3), (ii) observed RH and *T*, and (iii) the mixing ratios of organic compounds from the literatures (Table S1) (Wang et al., 2001; Wu et al., 2016; Rao et al., 2016).

Atmos. Chem. Phys. Discuss., https://doi.org/10.5194/acp-2018-334
Manuscript under review for journal Atmos. Chem. Phys.
Discussion started: 14 May 2018

Atmospheric Chemistry and Physics Discussions

3 Results and Discussion

3.1 Overview of observations in Beijing haze

Figure 3 describes general characteristics of haze events during our observations. The 12h-averaged $PM_{2.5}$ concentrations, corresponding with filter samples, varied from 16 to 323 μg m^{-3} with a mean of (141±88 (1σ)) μg m^{-3}. In comparison, the Grade II of NAAQS (National Ambient Air Quality Standard) in China is 75 μg m^{-3} for daily $PM_{2.5}$. The NO_3^- concentrations present similar trends with $PM_{2.5}$ levels (Fig. 3a), ranged from 0.3 to 106.7 μg m^{-3} with a mean of (6.1±5.3) μg m^{-3} in non-polluted days (NPD, $PM_{2.5} < 75$ μg m^{-3}) and (48.4±24.7) μg m^{-3} in polluted days (PD, $PM_{2.5} \geq 75$ μg m^{-3}). Correspondingly, the nitrogen oxidation ratio (NOR, which equals to NO_3^- molar concentration divided by the sum of NO_3^- and NO_2 molar concentration), a proxy for secondary transformation of nitrate (Sun et al., 2006), increased from a mean of (0.09±0.05) in NPD to (0.31±0.10) in PD (Fig. 3b). In residential heating season (Case III – IV in November 2014 – January 2015, Fig. 3b), Cl^- concentrations present similar trends with NO_3^- levels, increased from (0.6±1.0) μg m^{-3} in NPD to (7.9±4.8) μg m^{-3} in PD. However, during Case I – II in October 2014, Cl^- concentrations were (3.5±1.6) μg m^{-3} in NPD and (3.5±1.9) μg m^{-3} in PD, showing no significant difference at 0.01 level (t-test). Throughout our observational period, the visibility decreased from (11.4±6.7) km in NPD to (3.1±1.8) km in PD (Fig. 3c) while relative humidity (RH) increased from (37±12) % in NPD to (62±12) % in PD (Fig. 3d).

$\Delta^{17}O(NO_3^-)$ ranged from 27.5 ‰ to 33.9 ‰ with the mean of (29.1±1.3) ‰ in NPD and (31.0±1.7) ‰ in PD (Fig. 3c). Our observed $\Delta^{17}O(NO_3^-)$ is in the range of $\Delta^{17}O(NO_3^-)$ reported in literatures (Table 3) but at the high end of values from other non-polar regions (Table 3). All our observed $\Delta^{17}O(NO_3^-)$ values, no matter daytime sample (08:00 – 20:00) or nighttime sample (20:00 – 08:00), are larger than 24.85 ‰, the maximum of $\Delta^{17}O(NO_3^-)$ that can be produced via NO_2 + OH and NO_2 + H_2O at the assumption of $\Delta^{17}O(O_3)$ = 26 ‰ (Ishino et al., 2017; Vicars and Savarino, 2014). This directly suggests nocturnal formation pathways (N_2O_5 + H_2O/Cl^- and NO_3 + HC) must contribute to all the sampled nitrate. Given the lifetime of atmospheric nitrate is typically larger than our sampling collection interval (Vicars et al., 2013), each of our sample is expected to reflect both daytime and nocturnal nitrate production. Not surprisingly, $\Delta^{17}O(NO_3^-)$ mean of daytime and nighttime samples is (30.3±1.5) ‰ and (30.9±2.1) ‰, respectively, showing no significant difference at 0.01 level (t-test).

$\delta^{15}N(NO_3^-)$ in our observation varied from –2.5 ‰ to 19.2 ‰ with a mean of (7.4±6.8) ‰, which is in the range of $\delta^{15}N(NO_3^-)$ observed from rainwater in Beijing, China (Zhang et al., 2008) and similar to $\delta^{15}N(NO_3^-)$ values observed from aerosols in Germany (Freyer, 1991). Figure 3d shows that $\delta^{15}N(NO_3^-)$ varies largely in October 2014. The mean $\delta^{15}N(NO_3^-)$ varied from (0.4±1.5) ‰ in 08:00 Oct. 18 – 08:00 Oct. 21 to (10.7±1.4) ‰ in 08:00 Oct. 21 – 08:00 Oct. 23 and then

decreased to (–0.9±2.1) ‰ in 08:00 Oct. 23 – 08:00 Oct. 26, which corresponds to $PM_{2.5}$ concentrations being (155±63), (57±19) and (188±51) μg m^{-3} respectively. However, during residential heating season, relatively high $\delta^{15}N(NO_3^-)$ (7.6 – 19.2 ‰) were always observed both in NPD and PD.

3.2 Relationships between $\Delta^{17}O(NO_3^-)$ and other data

Figure 4 presents the relationships between $\Delta^{17}O(NO_3^-)$ and NO_3^- concentrations, $PM_{2.5}$ concentrations, NOR, visibility, RH and $\delta^{15}N(NO_3^-)$. $\Delta^{17}O(NO_3^-)$ shows an overall positive correlation with NO_3^- concentrations ($r = 0.55$, $p < 0.01$, Fig. 4a) and the correlation is better when $NO_3^- < 50$ μg m^{-3} ($r = 0.81$, $p < 0.01$). Similarly, $\Delta^{17}O(NO_3^-)$ shows an overall positive correlation with $PM_{2.5}$ concentration in Fig. 4b ($r = 0.64$, $p < 0.01$) and NOR in Fig. 4c ($r = 0.60$, $p < 0.01$), and their correlations are also better with samples featured by $NO_3^- < 50$ μg m^{-3} ($r = 0.71$ and $r = 0.80$, $p < 0.01$, respectively). Figure 4d shows that $\Delta^{17}O(NO_3^-)$ is negative correlated with visibility in general ($r = –0.66$, $p < 0.01$). The significant decrease of visibility will largely reduce surface radiation and thereby OH mixing ratios (Zheng et al., 2015b), which is unfavorable for nitrate production via NO_2 + OH pathway. Since NO_2 + OH pathway produces low $\Delta^{17}O(NO_3^-)$ (Table 1), the decreased importance of NO_2 + OH pathway will conversely increase $\Delta^{17}O(NO_3^-)$. Figure 4e shows that $\Delta^{17}O(NO_3^-)$ is positively correlated with RH in general ($r = 0.55$, $p < 0.01$). The raise of RH accompanying the large increase of $PM_{2.5}$ favors nitrate production via heterogeneous uptake of gases, e.g., N_2O_5 (Zheng et al., 2015b; Zheng et al., 2015a) and heterogeneous uptake of N_2O_5 produces relative high $\Delta^{17}O(NO_3^-)$ (Table 1), the enhanced heterogeneous uptake of N_2O_5 will increase $\Delta^{17}O(NO_3^-)$ too. Therefore, the decrease of importance of NO_2 + OH and the increase of importance of heterogeneous uptake of N_2O_5 should be responsible for the positive correlation between $\Delta^{17}O(NO_3^-)$ and NO_3^- concentrations. In addition, for samples with $NO_3^- > 50$ μg m^{-3}, visibility was always low with narrow variations (2.3±1.0 km) and RH was always high with narrow range (67±7 %), which may be responsible for the relatively high $\Delta^{17}O(NO_3^-)$ being observed (31.2±1.7 ‰). Figure 4f shows that $\Delta^{17}O(NO_3^-)$ is not correlated with $\delta^{15}N(NO_3^-)$, which has implications for the interpretation of $\delta^{15}N(NO_3^-)$. (See Sect. 3.4.2)

3.3 Estimate of nocturnal formation pathways

Before estimating the relative importance of different nitrate formation pathways, we estimate the proportion of O_3 oxidation in NO_X cycling, α. The possible α range can be calculated based on observed $\Delta^{17}O(NO_3^-)$. It can be obtained from Table 1 that 24.85α ‰ < $\Delta^{17}O(NO_3^-)$ < $(24.85\alpha + 13.66)$ ‰, so the lower limit of possible α is ($\Delta^{17}O(NO_3^-)$ – 13.66 ‰)/24.85 ‰. And since $\Delta^{17}O(NO_3^-) \geq 27.5$ ‰ in our observation, the higher limit of α is always 1 for all the samples. Figure 5 presents the possible range of calculated α based on $\Delta^{17}O(NO_3^-)$. The calculated lower limit of α ranged from 0.56 to 0.81 with a mean of (0.68±0.07), which directly suggests that O_3 oxidation played a dominated role in NO_X cycling during

Beijing haze. To estimate the specific α value, chemical kinetics in Table 2 and Eq. (3) were used. Specific α is estimated to range from 0.86 to 0.97 with a mean of (0.94±0.03), which is in the possible range of α value calculated directly based on $\Delta^{17}O(NO_3^-)$ and close to the range of 0.85 – 1 determined in other mid-latitude areas (Michalski et al., 2003; Patris et al., 2007).

Figure 6a shows the estimated relative importance of nocturnal formation pathways (N_2O_5 + H_2O/Cl^- and NO_3 + HC) during PD of each case on the basis of observed $\Delta^{17}O(NO_3^-)$. Possible fractional contribution of nocturnal formation pathways ranges from 49 – 97 %, 58 – 100 %, 60 – 100 %, 45 – 90 % and 70 – 100 % in PD of Case I to V, respectively, with a mean of 56 – 97 %. This directly implies that nocturnal chemistry dominates atmospheric nitrate production in Beijing haze. This finding is consistent with the suggested importance of heterogeneous uptake of N_2O_5 during Beijing haze by previous studies (Su et al., 2017; Wang et al., 2017b). The other pathways (NO_2 + OH and NO_2 + H_2O) account for the remaining fraction with a mean possible range of 3 – 44 %. Since NO_2 + OH and NO_2 + H_2O produces the same $\Delta^{17}O(NO_3^-)$ signature in our assumptions (Table 1), we cannot distinguish their fractional contribution barely from the observed $\Delta^{17}O(NO_3^-)$ in the present study. However, the overall positive correlation between $\Delta^{17}O(NO_3^-)$ and RH ($r = 0.55$, $p < 0.01$, Fig. 4e) suggests heterogeneous uptake of NO_2 should be less important than heterogeneous uptake of N_2O_5, otherwise, a negative relationship between $\Delta^{17}O(NO_3^-)$ and RH is expected. Our calculations also suggest that the sum of possible fractional contribution of N_2O_5 + Cl^- and NO_3 + HC is in the range of 0 – 49 %, 17 – 58 %, 20 – 60 %, 0 – 45 % and 41 – 70 % in PD of Case I to V, respectively, with a mean of 16 – 56 % (Table 4), which emphasizes that N_2O_5 + Cl^- and NO_3 + HC played a non-ignorable role in nitrate production during Beijing haze. Due to that N_2O_5 + Cl^- and NO_3 + HC produce the same $\Delta^{17}O(NO_3^-)$ in our assumptions (Table 1), we cannot distinguish their fractional contribution barely from the observed $\Delta^{17}O(NO_3^-)$ in this study, either. However, NO_3 + HC should be minor for nitrate production. For example, 3D modelling work of Alexander et al. (2009) suggests NO_3 + HC pathway only accounts for 4 % of global tropospheric nitrate production annually on average, and Michalski et al. (2003) found that NO_3 + HC pathway contributes 1 – 10 % to nitrate production on the basis of an annual observation at La Jolla, California, with low values in winter. Therefore, in addition to NO_3 + HC, N_2O_5 + Cl^- is likely to also contribute to nitrate production during haze in Beijing. Supportively, the concentrations of Cl^- is as high as (5.5±4.1) μg m^{-3} during PD of all the cases in our observation and the mixing ratios of $ClNO_2$, an indicator of N_2O_5 + Cl^- pathway, reached up to 2.9 nmol mol^{-1} during a summer observation in suburban Beijing (Wang et al., 2018b) and reached up to 5.0 nmol mol^{-1} in a modelling work in summer rural Beijing (Wang et al., 2017c).

Figure 6b presents the simulated mixing ratios of surface N_2O_5 and NO_3 radical during our observational period by using the box model MCM. The 12h averaged mixing ratios of simulated N_2O_5 ranged from 3 to 649 pmol mol^{-1} while simulated NO_3 radical ranged from 0 to 27 pmol mol^{-1}. In comparison, previous observations in Beijing suggest 5s averaged N_2O_5 can be as high as 1.3 nmol mol^{-1} and 30 min averaged NO_3 radical can be as high as 38 pmol mol^{-1} with large

day-to-day variability (Wang et al., 2017b; Wang et al., 2015). During Case I and II in October, simulated N_2O_5 and NO_3 radical present similar trends with the observed NO_3^- and remain relatively high during PD (346±128 pmol mol^{-1} and 9±7 pmol mol^{-1}, respectively, Fig. 6b), which supports the dominant role of nocturnal formation pathways suggested by $\Delta^{17}O(NO_3^-)$. However, during Case III – V in residential heating season, the simulated surface mixing ratios of N_2O_5 and NO_3 radical remain relatively low during PD (63±80 pmol mol^{-1} and < 1 pmol mol^{-1}, respectively, Fig. 6b), which seems to be inconsistent with $\Delta^{17}O(NO_3^-)$ observations. We note that a recent study suggests that heterogeneous uptake of N_2O_5 is negligible at surface but larger at higher altitudes (e.g., > 150 m) during winter haze in Beijing (Wang et al., 2018a). So during PD of Case III – V in our observational period, large nitrate production via heterogeneous uptake of N_2O_5 may occur aloft rather than at surface, which leads to the dominant role of nocturnal formation pathways as suggested by $\Delta^{17}O(NO_3^-)$.

3.4 Interpretation of $\delta^{15}N(NO_3^-)$ variations

The variation of atmospheric $\delta^{15}N(NO_3^-)$ can be interpreted by the following four processes (Vicars et al., 2013): (i) variations in $\delta^{15}N$ signature of NO_X sources; (ii) isotopic exchange between NO and NO_2; (iii) isotopic fractionations associated with nitrate formation pathways; and (iv) isotopic effects occurring during transport, such as deposition of NO_3^- and HNO_3 partitioning between gas and particle phase. So far there remains large uncertainties to quantify the contribution of above processes to variations of atmospheric $\delta^{15}N(NO_3^-)$, therefore, we focus on qualitatively discussing potential influence of the above four processes on the observed $\delta^{15}N(NO_3^-)$ as follows.

3.4.1 Isotopic effects occurring during transport

One key process that possibly changes $\delta^{15}N(NO_3^-)$ during transport is wet deposition, i.e., washout of atmospheric nitrate by rain. However, field observations suggest wet deposition of nitrate can either lead to enrichment (Freyer, 1991) or depletion of the remaining atmospheric $\delta^{15}N(NO_3^-)$ (Baker et al., 2007), which renders difficult in estimating the influence of wet deposition. Nevertheless, throughout our sampling period, no rains were observed except for a small snow lasted for 2 h from 23: 00 Dec. 9 to 1:00 Dec. 10. Therefore, the role of wet deposition in $\delta^{15}N(NO_3^-)$ variations should be negligible during our observations. For the influence of HNO_3 partitioning between gas and particle phase, previous studies have shown that particulate nitrate is enriched in $\delta^{15}N$ relative to gaseous HNO_3 (Freyer, 1991). However, as the quartz filter used here is thought to collect both particulate nitrate and gaseous HNO_3 (Vicars et al., 2013; Morin et al., 2009), we assume the influence of HNO_3 partitioning between gas and particle phase on $\delta^{15}N(NO_3^-)$ variations is minor in our observations.

3.4.2 Isotopic fractionations associated with nitrate formation pathways

It has been proposed that atmospheric nitrate that resulting from heterogeneous uptake of N_2O_5 is enriched in $\delta^{15}N$

while nitrate resulting from NO_2 + OH pathway is depleted in $\delta^{15}N$ (Freyer, 1991), which means $\delta^{15}N(NO_3^-)$ will vary in the same way with $\Delta^{17}O(NO_3^-)$, e.g., higher contribution from heterogeneous uptake of N_2O_5 and lower contribution from NO_2 + OH tends to result in both higher $\Delta^{17}O(NO_3^-)$ and $\delta^{15}N(NO_3^-)$, if the influence of isotopic fractionations associated with nitrate formation pathways is a main factor for the variations of $\delta^{15}N(NO_3^-)$. However, $\delta^{15}N(NO_3^-)$ don't present similar trends with $\Delta^{17}O(NO_3^-)$ in our observations (Fig. 3d and Fig. 4f). Especially for Case I and II in October, it's believed that relative importance of heterogeneous uptake of N_2O_5 increases and NO_2 + OH decreases from NPD to PD, on the basis that our observed $\Delta^{17}O(NO_3^-)$ (Fig. 1c) and simulated N_2O_5 mixing ratios (Fig. 6b) increases from NPD to PD while previous studies modelled OH mixing ratio decrease from NPD to PD (Rao et al., 2016; Zheng et al., 2015a), however, atmospheric $\delta^{15}N(NO_3^-)$ was observed to decrease largely from (10.0±0.7) ‰ in NPD to (0.7±4.0) ‰ in PD instead of an increase. Therefore isotopic fractionations associated with nitrate formation pathways is not likely to be a significant factor for the variation of $\delta^{15}N(NO_3^-)$ during our observations, especially for the large variations of $\delta^{15}N(NO_3^-)$ in October. In other words, the main variation of $\delta^{15}N(NO_3^-)$ should have been already established before nitrate formation.

3.4.3 Isotopic exchange between NO and NO_2

The quantitative effect of isotopic exchange in terms of $\delta^{15}N$ difference between NO_2 and NO_X sources has been proposed as Eq. (6) (Freyer et al., 1993).

$$[\delta^{15}N(NO_2) - \delta^{15}N(NO_X)] = (K - 1) \times (1 - f_{NO_2}) \quad (6)$$

Where K is the isotopic exchange constant of N between NO and NO_2, which is temperature-dependent (Walters et al., 2016), and f_{NO2} is the mole fraction of NO_2 to NO_X.

Figure 7a shows the relationship between observed $\delta^{15}N(NO_3^-)$ and calculated $[\delta^{15}N(NO_2) - \delta^{15}N(NO_X)]$ during our sampling period. $\delta^{15}N(NO_3^-)$ shows an overall positive correlation with $[\delta^{15}N(NO_2) - \delta^{15}N(NO_X)]$ ($r = 0.54$, $p < 0.01$, Fig. 7a) and the correlation is better in residential heating season ($r = 0.69$, $p < 0.01$), indicating that the isotopic exchange between NO and NO_2 is likely to be an important factor for the variations of $\delta^{15}N(NO_3^-)$, especially in residential heating season. This finding, along with previous reports that the isotopic exchange between NO and NO_2 can contribute to seasonal variations of $\delta^{15}N(NO_3^-)$ (Freyer et al., 1993), have implications for the interpretation of $\delta^{15}N(NO_3^-)$ observations. As shown in Eq. (6), NO_2 may become gradually enriched in $\delta^{15}N$ over NO_X along with the decrease of f_{NO2}, resulting in the increase of $\delta^{15}N(NO_3^-)$. In this case, a higher $\delta^{15}N(NO_3^-)$ value does not directly reflect a larger contribution from anthropogenic sources. $\delta^{15}N(NO_3^-)$ should therefore be interpreted with the consideration of atmospheric contexts (Vicars et al., 2013).

3.4.4 Influence of NO_X emissions

It shows in Fig. 7a that $\delta^{15}N(NO_3^-)$ is not significantly correlated with $[\delta^{15}N(NO_2) - \delta^{15}N(NO_X)]$ in October, which

leaves influence of NO_X sources being the most possible cause for the large variation of $\delta^{15}N(NO_3^-)$ in October. We note that the mass ratio of Cl^-/NO_3^- presents a strongly positive correlation with $\delta^{15}N(NO_3^-)$ in October ($r = 0.94$, $p < 0.01$, Fig. 7b). Since Cl^- in fine aerosol is mainly from coal combustion in Beijing and its surrounding regions (Tham et al., 2016), the strong correlation between Cl^-/NO_3^- and $\delta^{15}N(NO_3^-)$ indicates the relative importance of coal combustion is likely to play a main role in $\delta^{15}N(NO_3^-)$ variations in October. In residential heating season, Cl^-/NO_3^- also presents a positive correlation with $\delta^{15}N(NO_3^-)$ ($r = 0.64$, $p = 0.01$, Fig. 7b), which also emphasize the importance of coal combustion in $\delta^{15}N(NO_3^-)$ variations. Previous work has suggested that NO_X emissions are predominated by anthropogenic sources (e.g., coal combustion and vehicles) in north China (Wang et al., 2012; Lin, 2012) with coal combustion being the largest contributor (Zhang et al., 2007). Furthermore, coal combustion is suggested to generally have the highest $\delta^{15}N(NO_X)$ value compare to other anthropogenic sources such vehicles (Felix et al., 2012). Therefore the variations of the relative importance of NO_X emissions from coal combustion should have significant impact on atmospheric $\delta^{15}N(NO_3^-)$ in Beijing.

4 Conclusions

We report the first observation of isotopic composition ($\Delta^{17}O$ and $\delta^{15}N$) of atmospheric nitrate in Beijing haze. The observed $\Delta^{17}O(NO_3^-)$ ranged from 27.5 to 33.9 ‰ with a mean of (30.6±1.8) ‰ while $\delta^{15}N(NO_3^-)$ ranged largely from –2.5 to 19.2 ‰ with a mean of (7.4±6.8) ‰. A positive correlation between $\Delta^{17}O(NO_3^-)$ and NO_3^- concentration was observed ($r = 0.81$, $p < 0.01$) when $NO_3^- < 50$ μg m^{-3}, which is likely to result from the variation of relative importance of different nitrate formation pathway. Calculations with the constraint of $\Delta^{17}O(NO_3^-)$ suggest nocturnal pathways ($N_2O_5 + H_2O/Cl^-$ and $NO_3 + HC$) dominated nitrate production during polluted days ($PM_{2.5} \geq 75$ μg m^{-3}) with the mean possible contribution of 56 – 97 %. $\Delta^{17}O(NO_3^-)$ also indicates that O_3 oxidation played a dominated role in NO_X cycling during Beijing haze. Data analysis of atmospheric $\delta^{15}N(NO_3^-)$ shows that its main variation should have been already established before nitrate formation in our observations. A combined effect of isotopic exchange between NO and NO_2 and variability in the relative importance of coal combustion emitted NO_X was found to be most responsible for $\delta^{15}N(NO_3^-)$ variations.

Data availability

All data needed to draw the conclusions are present in the main text and/or the Supplementary Materials. For additional data, please contact the corresponding author (zqxie@ustc.edu.cn).

Author contributions

Z.Q.X. conceived this study. P.Z.H. conducted isotope measurements. P.Z.H., X.Y.C, S.D.F., H.C.Z., H. K. performed the field experiments and ion measurements. P.Z.H., Z.Q.X., X.W.Y. interpreted the data. C.L. contributed to the field observation support. P.Z.H. wrote the manuscript with Z.Q.X. inputs. All authors involved the discussion and revision.

Competing interests

The authors declare no competing interests.

Acknowledgments

This work was supported by the National Key Project of MOST (2016YFC0203302), NSFC (91544013), the Key Project of CAS (KJZD-EW-TZ-G06-01) and the Atmospheric Pollution Control of the Prime Minister (DQGG0104). We gratefully thank staffs of IsoLab at UW for their technical support and Becky Alexander for helpful discussions.

References

Alexander, B., Hastings, M. G., Allman, D. J., Dachs, J., Thornton, J. A., and Kunasek, S. A.: Quantifying atmospheric nitrate formation pathways based on a global model of the oxygen isotopic composition (Δ17O) of atmospheric nitrate, Atmos. Chem. Phys., 9, 5043-5056, 2009.

Baker, A. R., Weston, K., Kelly, S. D., Voss, M., Streu, P., and Cape, J. N.: Dry and wet deposition of nutrients from the tropical Atlantic atmosphere: Links to primary productivity and nitrogen fixation, Deep Sea Res. Part I, 54, 1704-1720, 2007.

Berhanu, T. A., Savarino, J., Bhattacharya, S. K., and Vicars, W. C.: 17O excess transfer during the NO2 + O3 → NO3 + O2 reaction, J. Chem. Phys., 136, 044311, 2012.

334 Bertram, T. H., and Thornton, J. A.: Toward a general parameterization of N2O5 reactivity on aqueous particles: the
335 competing effects of particle liquid water, nitrate and chloride, Atmos. Chem. Phys., 9, 8351-8363, 2009.
336 Beyn, F., Matthias, V., and Dähnke, K.: Changes in atmospheric nitrate deposition in Germany–An isotopic perspective,
337 Environ. Pollut., 194, 1-10, 2014.
338 Brenninkmeijer, C. A., Janssen, C., Kaiser, J., Röckmann, T., Rhee, T. S., and Assonov, S. S.: Isotope effects in the chemistry
339 of atmospheric trace compounds, Chem. Rev., 103, 5125-5162, 2003.
340 Brook, R. D., Rajagopalan, S., Pope, C. A., Brook, J. R., Bhatnagar, A., Diez-Roux, A. V., Holguin, F., Hong, Y., Luepker, R.
341 V., and Mittleman, M. A.: Particulate matter air pollution and cardiovascular disease an update to the scientific
342 statement from the American Heart Association, Circulation, 121, 2331-2378, 2010.
343 Brown, S. S., and Stutz, J.: Nighttime radical observations and chemistry, Chem. Soc. Rev., 41, 6405-6447, 2012.
344 Burkholder, J. B., Sander, S. P., Abbatt, J. P. D., Barker, J. R., Huie, R. E., Kolb, C. E., Kurylo, M. J., Orkin, V. L., Wilmouth,
345 D. M., and Wine, P. H.: Chemical Kinetics and Photochemical Data for Use in Atmospheric Studies: Evaluation
346 Number 18, Pasadena, CA: Jet Propulsion Laboratory, National Aeronautics and Space Administration, 2015.
347 Chen, Q., Geng, L., Schmidt, J. A., Xie, Z., Kang, H., Dachs, J., Cole-Dai, J., Schauer, A. J., Camp, M. G., and Alexander, B.:
348 Isotopic constraints on the role of hypohalous acids in sulfate aerosol formation in the remote marine boundary layer,
349 Atmos. Chem. Phys., 16, 11433-11450, 2016.
350 Chen, Z., Zhang, J., Zhang, T., Liu, W., and Liu, J.: Haze observations by simultaneous lidar and WPS in Beijing before and
351 during APEC, 2014, Sci. China Chem., 58, 1385-1392, 2015.
352 Cheng, Z., Jiang, J., Fajardo, O., Wang, S., and Hao, J.: Characteristics and health impacts of particulate matter pollution in
353 China (2001–2011), Atmos. Environ., 65, 186-194, 2013.
354 Cheung, J. L., Li, Y., Boniface, J., Shi, Q., Davidovits, P., Worsnop, D. R., Jayne, J. T., and Kolb, C. E.: Heterogeneous
355 interactions of NO2 with aqueous surfaces, J. Phys. Chem. A, 104, 2655-2662, 2000.
356 Elliott, E. M., Kendall, C., Boyer, E. W., Burns, D. A., Lear, G. G., Golden, H. E., Harlin, K., Bytnerowicz, A., Butler, T. J.,
357 and Glatz, R.: Dual nitrate isotopes in dry deposition: Utility for partitioning NOx source contributions to landscape
358 nitrogen deposition, J. Geophys. Res. Biogeo., 114, 2009.
359 Elshorbany, Y. F., Kleffmann, J., Hofzumahaus, A., Kurtenbach, R., Wiesen, P., Brauers, T., Bohn, B., Dorn, H. P., Fuchs, H.,
360 and Holland, F.: HOx budgets during HOxComp: A case study of HOx chemistry under NOx - limited conditions, J.
361 Geophys. Res., 117, 2012.
362 Fang, Y., Koba, K., Wang, X., Wen, D., Li, J., Takebayashi, Y., Liu, X., and Yoh, M.: Anthropogenic imprints on nitrogen and
363 oxygen isotopic composition of precipitation nitrate in a nitrogen-polluted city in southern China, Atmos. Chem. Phys.,
364 11, 1313-1325, 2011.

365 Felix, J. D., Elliott, E. M., and Shaw, S. L.: Nitrogen isotopic composition of coal-fired power plant NOx: influence of
366 emission controls and implications for global emission inventories, Environ. Sci. Technol., 46, 3528-3535, 2012.
367 Freyer, H. D.: Seasonal variation of 15N/14N ratios in atmospheric nitrate species, Tellus B, 43, 30-44, 1991.
368 Freyer, H. D., Kley, D., Volz‐Thomas, A., and Kobel, K.: On the interaction of isotopic exchange processes with
369 photochemical reactions in atmospheric oxides of nitrogen, J. Geophys. Res. Atmos., 98, 14791-14796, 1993.
370 Goodman, A. L., Underwood, G. M., and Grassian, V. H.: Heterogeneous reaction of NO2: Characterization of gas-phase
371 and adsorbed products from the reaction, 2NO2(g) + H2O(a) → HONO(g) + HNO3(a) on hydrated silica particles, J.
372 Phys. Chem. A, 103, 7217-7223, 1999.
373 Guha, T., Lin, C. T., Bhattacharya, S. K., Mahajan, A. S., Ou-Yang, C.-F., Lan, Y.-P., Hsu, S. C., and Liang, M.-C.: Isotopic
374 ratios of nitrate in aerosol samples from Mt. Lulin, a high-altitude station in Central Taiwan, Atmos. Environ., 154,
375 53-69, 2017.
376 Hastings, M. G., Casciotti, K. L., and Elliott, E. M.: Stable isotopes as tracers of anthropogenic nitrogen sources, deposition,
377 and impacts, Elements, 9, 339-344, 2013.
378 He, P., Alexander, B., Geng, L., Chi, X., Fan, S., Zhan, H., Kang, H., Zheng, G., Cheng, Y., Su, H., Liu, C., and Xie, Z.:
379 Isotopic constraints on heterogeneous sulphate production in Beijing haze, Atmos. Chem. Phys. Discuss., 1-25, 2017.
380 Hoering, T.: The isotopic composition of the ammonia and the nitrate ion in rain, Geochim. Cosmochim. Acta, 12, 97-102,
381 1957.
382 Ishino, S., Hattori, S., Savarino, J., Jourdain, B., Preunkert, S., Legrand, M., Caillon, N., Barbero, A., Kuribayashi, K., and
383 Yoshida, N.: Seasonal variations of triple oxygen isotopic compositions of atmospheric sulfate, nitrate, and ozone at
384 Dumont d'Urville, coastal Antarctica, Atmos. Chem. Phys., 17, 3713-3727, 2017.
385 Kaiser, J., Hastings, M. G., Houlton, B. Z., Röckmann, T., and Sigman, D. M.: Triple oxygen isotope analysis of nitrate using
386 the denitrifier method and thermal decomposition of N2O, Anal. Chem., 79, 599-607, 2007.
387 Kanaya, Y., Cao, R., Akimoto, H., Fukuda, M., Komazaki, Y., Yokouchi, Y., Koike, M., Tanimoto, H., Takegawa, N., and
388 Kondo, Y.: Urban photochemistry in central Tokyo: 1. Observed and modeled OH and HO2 radical concentrations
389 during the winter and summer of 2004, J. Geophys. Res., 112, 2007.
390 Kunasek, S. A., Alexander, B., Steig, E. J., Hastings, M. G., Gleason, D. J., and Jarvis, J. C.: Measurements and modeling of
391 Δ17O of nitrate in snowpits from Summit, Greenland, J. Geophys. Res., 113, 2008.
392 Li, H., Zhu, T., Zhao, D., Zhang, Z., and Chen, Z.: Kinetics and mechanisms of heterogeneous reaction of NO2 on CaCO3
393 surfaces under dry and wet conditions, Atmos. Chem. Phys., 10, 463-474, 2010.
394 Li, Z., Hu, R., Xie, P., Wang, H., Lu, K., and Wang, D.: Intercomparison of in situ CRDS and CEAS for measurements of
395 atmospheric N2O5 in Beijing, China, Sci. Total Environ., 613, 131-139, 2018.

396 Lin, J.-T.: Satellite constraint for emissions of nitrogen oxides from anthropogenic, lightning and soil sources over East
397 China on a high-resolution grid, Atmos. Chem. Phys., 12, 2881-2898, 2012.
398 Lin, W., Xu, X., Ge, B., and Liu, X.: Gaseous pollutants in Beijing urban area during the heating period 2007–2008:
399 variability, sources, meteorological, and chemical impacts, Atmos. Chem. Phys., 11, 8157-8170, 2011.
400 Liu, Z., Wang, Y., Gu, D., Zhao, C., Huey, L., Stickel, R., Liao, J., Shao, M., Zhu, T., and Zeng, L.: Summertime
401 photochemistry during CAREBeijing-2007: ROx budgets and O3 formation, Atmos. Chem. Phys., 12, 7737-7752,
402 2012.
403 Michalski, G., Scott, Z., Kabiling, M., and Thiemens, M. H.: First measurements and modeling of Δ17O in atmospheric
404 nitrate, Geophys. Res. Lett., 30, 2003.
405 Mihelcic, D., Holland, F., Hofzumahaus, A., Hoppe, L., Konrad, S., Müsgen, P., Pätz, H. W., Schäfer, H. J., Schmitz, T., and
406 Volz‐Thomas, A.: Peroxy radicals during BERLIOZ at Pabstthum: Measurements, radical budgets and ozone
407 production, J. Geophys. Res., 108, 2003.
408 Morin, S., Savarino, J., Bekki, S., Cavender, A., Shepson, P. B., and Bottenheim, J. W.: Major influence of BrO on the NOx
409 and nitrate budgets in the Arctic spring, inferred from Δ17O(NO3–) measurements during ozone depletion events,
410 Environ. Chem., 4, 238, 2007a.
411 Morin, S., Savarino, J., Bekki, S., Gong, S., and Bottenheim, J. W.: Signature of Arctic surface ozone depletion events in the
412 isotope anomaly (Δ17O) of atmospheric nitrate, Atmos. Chem. Phys., 7, 1451-1469, 2007b.
413 Morin, S., Savarino, J., Frey, M. M., Yan, N., Bekki, S., Bottenheim, J. W., and Martins, J. M.: Tracing the origin and fate of
414 NOx in the Arctic atmosphere using stable isotopes in nitrate, Science, 322, 730-732, 2008.
415 Morin, S., Savarino, J., Frey, M. M., Domine, F., Jacobi, H. W., Kaleschke, L., and Martins, J. M.: Comprehensive isotopic
416 composition of atmospheric nitrate in the Atlantic Ocean boundary layer from 65 S to 79 N, J. Geophys. Res. Atmos.,
417 114, 2009.
418 Morin, S., Sander, R., and Savarino, J.: Simulation of the diurnal variations of the oxygen isotope anomaly (Δ17O) of
419 reactive atmospheric species, Atmos. Chem. Phys., 11, 3653-3671, 2011.
420 Pathak, R. K., Wu, W. S., and Wang, T.: Summertime PM2.5 ionic species in four major cities of China: nitrate formation in
421 an ammonia-deficient atmosphere, Atmos. Chem. Phys., 9, 1711-1722, 2009.
422 Pathak, R. K., Wang, T., and Wu, W. S.: Nighttime enhancement of PM2.5 nitrate in ammonia-poor atmospheric conditions
423 in Beijing and Shanghai: plausible contributions of heterogeneous hydrolysis of N2O5 and HNO3 partitioning, Atmos.
424 Environ., 45, 1183-1191, 2011.
425 Patris, N., Cliff, S. S., Quinn, P. K., Kasem, M., and Thiemens, M. H.: Isotopic analysis of aerosol sulfate and nitrate during
426 ITCT‐2k2: Determination of different formation pathways as a function of particle size, J. Geophys. Res. Atmos., 112,

2007.

Rao, Z., Chen, Z., Liang, H., Huang, L., and Huang, D.: Carbonyl compounds over urban Beijing: Concentrations on haze and non-haze days and effects on radical chemistry, Atmos. Environ., 124, 207-216, 2016.

Savarino, J., and Thiemens, M. H.: Analytical procedure to determine both δ18O and δ17O of H2O2 in natural water and first measurements, Atmos. Environ., 33, 3683-3690, 1999.

Savarino, J., Kaiser, J., Morin, S., Sigman, D. M., and Thiemens, M. H.: Nitrogen and oxygen isotopic constraints on the origin of atmospheric nitrate in coastal Antarctica, Atmos. Chem. Phys., 7, 1925-1945, 2007.

Savarino, J., Bhattacharya, S. K., Morin, S., Baroni, M., and Doussin, J.-F.: The NO + O3 reaction: A triple oxygen isotope perspective on the reaction dynamics and atmospheric implications for the transfer of the ozone isotope anomaly, J. Chem. Phys., 128, 194303, 2008.

Savarino, J., Morin, S., Erbland, J., Grannec, F., Patey, M. D., Vicars, W., Alexander, B., and Achterberg, E. P.: Isotopic composition of atmospheric nitrate in a tropical marine boundary layer, P. Natl. Acad. Sci. USA, 110, 17668-17673, 2013.

Sofen, E. D., Alexander, B., Steig, E. J., Thiemens, M. H., Kunasek, S. A., Amos, H. M., Schauer, A. J., Hastings, M. G., Bautista, J., and Jackson, T. L.: WAIS Divide ice core suggests sustained changes in the atmospheric formation pathways of sulfate and nitrate since the 19th century in the extratropical Southern Hemisphere, Atmos. Chem. Phys., 14, 5749-5769, 2014.

Su, X., Tie, X., Li, G., Cao, J., Huang, R., Feng, T., Long, X., and Xu, R.: Effect of hydrolysis of N2O5 on nitrate and ammonium formation in Beijing China: WRF-Chem model simulation, Sci. Total Environ., 579, 221-229, 2017.

Sun, Y., Zhuang, G., Tang, A., Wang, Y., and An, Z.: Chemical characteristics of PM2.5 and PM10 in haze-fog episodes in Beijing, Environ. Sci. Technol., 40, 3148-3155, 2006.

Tham, Y. J., Wang, Z., Li, Q., Yun, H., Wang, W., Wang, X., Xue, L., Lu, K., Ma, N., Bohn, B., Li, X., Kecorius, S., Größ, J., Shao, M., Wiedensohler, A., Zhang, Y., and Wang, T.: Significant concentrations of nitryl chloride sustained in the morning: investigations of the causes and impacts on ozone production in a polluted region of northern China, Atmos. Chem. Phys., 16, 14959-14977, 2016.

Tong, S., Hou, S., Zhang, Y., Chu, B., Liu, Y., He, H., Zhao, P., and Ge, M.: Comparisons of measured nitrous acid (HONO) concentrations in a pollution period at urban and suburban Beijing, in autumn of 2014, Sci. China Chem., 58, 1393-1402, 2015.

Vicars, W. C., Morin, S., Savarino, J., Wagner, N. L., Erbland, J., Vince, E., Martins, J. M. F., Lerner, B. M., Quinn, P. K., and Coffman, D. J.: Spatial and diurnal variability in reactive nitrogen oxide chemistry as reflected in the isotopic composition of atmospheric nitrate: Results from the CalNex 2010 field study, J. Geophys. Res. Atmos., 118, 2013.

458 Vicars, W. C., and Savarino, J.: Quantitative constraints on the 17O-excess (Δ17O) signature of surface ozone: Ambient
459 measurements from 50 ºN to 50 ºS using the nitrite-coated filter technique, Geochim. Cosmochim. Acta, 135, 270-287,
460 2014.
461 Walters, W. W., Simonini, D. S., and Michalski, G.: Nitrogen isotope exchange between NO and NO2 and its implications
462 for δ15N variations in tropospheric NOx and atmospheric nitrate, Geophys. Res. Lett., 43, 440-448, 2016.
463 Wang, D., Hu, R., Xie, P., Liu, J., Liu, W., Qin, M., Ling, L., Zeng, Y., Chen, H., Xing, X., Zhu, G., Wu, J., Duan, J., Lu, X.,
464 and Shen, L.: Diode laser cavity ring-down spectroscopy for in situ measurement of NO3 radical in ambient air, J.
465 Quant. Spectrosc. Radiat. Transf., 166, 23-29, 2015.
466 Wang, H., Chen, J., and Lu, K.: Development of a portable cavity-enhanced absorption spectrometer for the measurement of
467 ambient NO3 and N2O5: experimental setup, lab characterizations, and field applications in a polluted urban
468 environment, Atmos. Meas. Tech., 10, 1465, 2017a.
469 Wang, H., Lu, K., Chen, X., Zhu, Q., Chen, Q., Guo, S., Jiang, M., Li, X., Shang, D., and Tan, Z.: High N2O5 concentrations
470 observed in urban Beijing: Implications of a large nitrate formation pathway, Environ. Sci. Technol. Lett., 4, 416-420,
471 2017b.
472 Wang, H., Lu, K., Tan, Z., Sun, K., Li, X., Hu, M., Shao, M., Zeng, L., Zhu, T., and Zhang, Y.: Model simulation of NO3,
473 N2O5 and ClNO2 at a rural site in Beijing during CAREBeijing-2006, Atmos. Res., 196, 97-107, 2017c.
474 Wang, H., Lu, K., Chen, X., Zhu, Q., Wu, Z., Wu, Y., and Sun, K.: Large particulate nitrate formation from N2O5 uptake in a
475 chemically reactive layer aloft during wintertime in Beijing, Atmos. Chem. Phys. Discuss., 1-27, 2018a.
476 Wang, H., Lu, K., Guo, S., Wu, Z., Shang, D., Tan, Z., Wang, Y., Le Breton, M., Zhu, W., Lou, S., Tang, M., Wu, Y., Zheng,
477 J., Zeng, L., Hallquist, M., Hu, M., and Zhang, Y.: Efficient N2O5 Uptake and NO3 Oxidation in the Outflow of Urban
478 Beijing, Atmos. Chem. Phys. Discuss., 1-27, 2018b.
479 Wang, J., Zhang, X., Guo, J., Wang, Z., and Zhang, M.: Observation of nitrous acid (HONO) in Beijing, China: Seasonal
480 variation, nocturnal formation and daytime budget, Sci. Total Environ., 587, 350-359, 2017d.
481 Wang, S., Zhang, Q., Streets, D. G., He, K., Martin, R. V., Lamsal, L. N., Chen, D., Lei, Y., and Lu, Z.: Growth in NOx
482 emissions from power plants in China: bottom-up estimates and satellite observations, Atmos. Chem. Phys., 12,
483 4429-4447, 2012.
484 Wang, Y., Zhou, L., Wang, M., and Zheng, X.: Trends of atmospheric methane in Beijing, Chemosphere, 3, 65-71, 2001.
485 Wen, L., Chen, J., Yang, L., Wang, X., Xu, C., Sui, X., Yao, L., Zhu, Y., Zhang, J., and Zhu, T.: Enhanced formation of fine
486 particulate nitrate at a rural site on the North China Plain in summer: The important roles of ammonia and ozone, Atmos.
487 Environ., 101, 294-302, 2015.
488 Wu, R., Li, J., Hao, Y., Li, Y., Zeng, L., and Xie, S.: Evolution process and sources of ambient volatile organic compounds

during a severe haze event in Beijing, China, Sci. Total Environ., 560, 62-72, 2016.

Xiao, H., Xie, L., Long, A., Ye, F., Pan, Y., Li, D., Long, Z., Chen, L., Xiao, H., and Liu, C.: Use of isotopic compositions of nitrate in TSP to identify sources and chemistry in South China Sea, Atmos. Environ., 109, 70-78, 2015.

Xu, X., Zhao, W., Zhang, Q., Wang, S., Fang, B., Chen, W., Venables, D. S., Wang, X., Pu, W., and Wang, X.: Optical properties of atmospheric fine particles near Beijing during the HOPE-J3 A campaign, Atmos. Chem. Phys., 16, 6421-6439, 2016.

Ye, P., Xie, Z., Yu, J., and Kang, H.: Spatial distribution of methanesulphonic acid in the Arctic aerosol collected during the Chinese Arctic Research Expedition, Atmosphere, 6, 699-712, 2015.

Yu, Z., and Elliott, E. M.: Novel Method for Nitrogen Isotopic Analysis of Soil-Emitted Nitric Oxide, Environ. Sci. Technol., 2017.

Zhang, J., Chen, Z., Lu, Y., Gui, H., Liu, J., Liu, W., Wang, J., Yu, T., Cheng, Y., and Chen, Y.: Characteristics of aerosol size distribution and vertical backscattering coefficient profile during 2014 APEC in Beijing, Atmos. Environ., 148, 30-41, 2017.

Zhang, Q., Streets, D. G., He, K., Wang, Y., Richter, A., Burrows, J. P., Uno, I., Jang, C. J., Chen, D., Yao, Z., and Lei, Y.: NOx emission trends for China, 1995–2004: The view from the ground and the view from space, J. Geophys. Res., 112, 2007.

Zhang, Y., Liu, X., Fangmeier, A., Goulding, K. T. W., and Zhang, F.: Nitrogen inputs and isotopes in precipitation in the North China Plain, Atmos. Environ., 42, 1436-1448, 2008.

Zheng, B., Zhang, Q., Zhang, Y., He, K., Wang, K., Zheng, G., Duan, F., Ma, Y., and Kimoto, T.: Heterogeneous chemistry: a mechanism missing in current models to explain secondary inorganic aerosol formation during the January 2013 haze episode in North China, Atmos. Chem. Phys., 15, 2031-2049, 2015a.

Zheng, G., Duan, F., Su, H., Ma, Y., Cheng, Y., Zheng, B., Zhang, Q., Huang, T., Kimoto, T., and Chang, D.: Exploring the severe winter haze in Beijing: the impact of synoptic weather, regional transport and heterogeneous reactions, Atmos. Chem. Phys., 15, 2969-2983, 2015b.

Atmos. Chem. Phys. Discuss., https://doi.org/10.5194/acp-2018-334
Manuscript under review for journal Atmos. Chem. Phys.
Discussion started: 14 May 2018

Atmospheric Chemistry and Physics Discussions

513 **Figures and Tables**

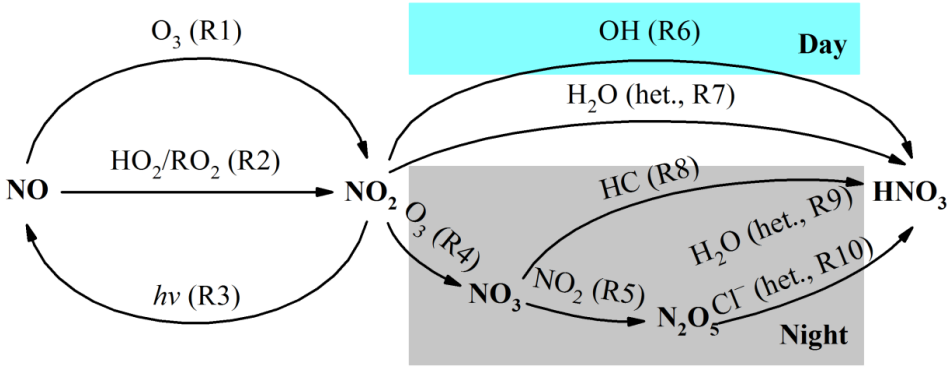

514

515 **Figure 1.** Simplified schematic of the main nitrate formation pathways in urban air. "het." means heterogeneous reactions on

516 aerosols.

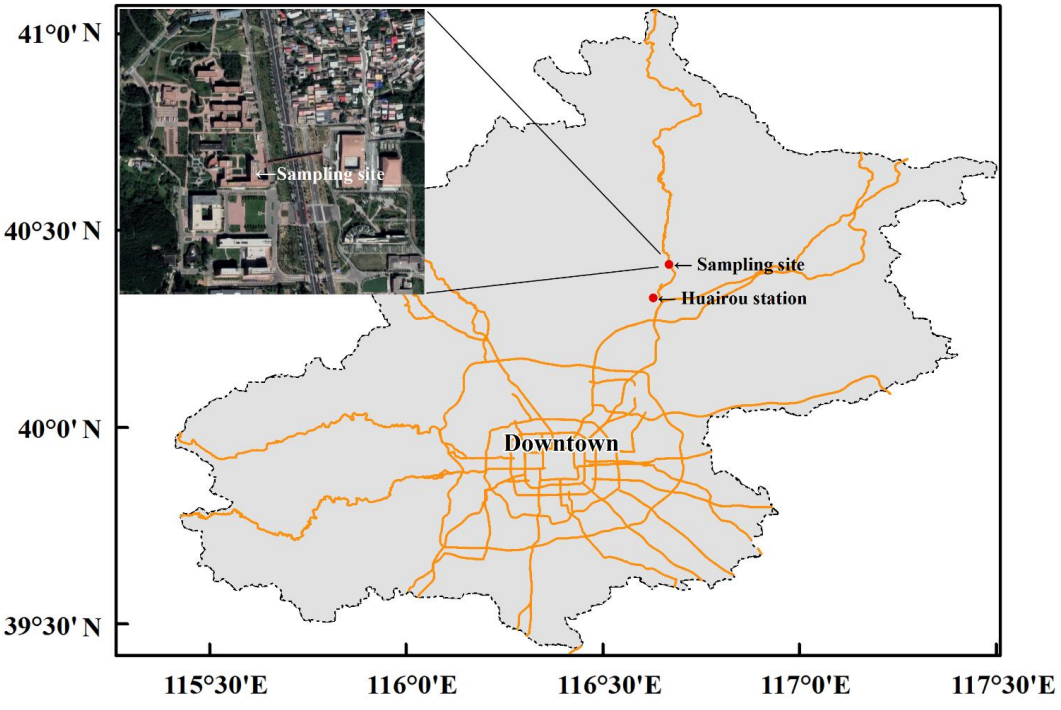

517

518 **Figure 2.** A brief map of sampling site in Beijing. The map scale of base map is 1:1250000. Huairou station is set by Beijing

519 Municipal Environmental Monitoring Center, where hourly $PM_{2.5}$, SO_2, CO, NO_2 and O_3 were observed.

Atmos. Chem. Phys. Discuss., https://doi.org/10.5194/acp-2018-334
Manuscript under review for journal Atmos. Chem. Phys.
Discussion started: 14 May 2018

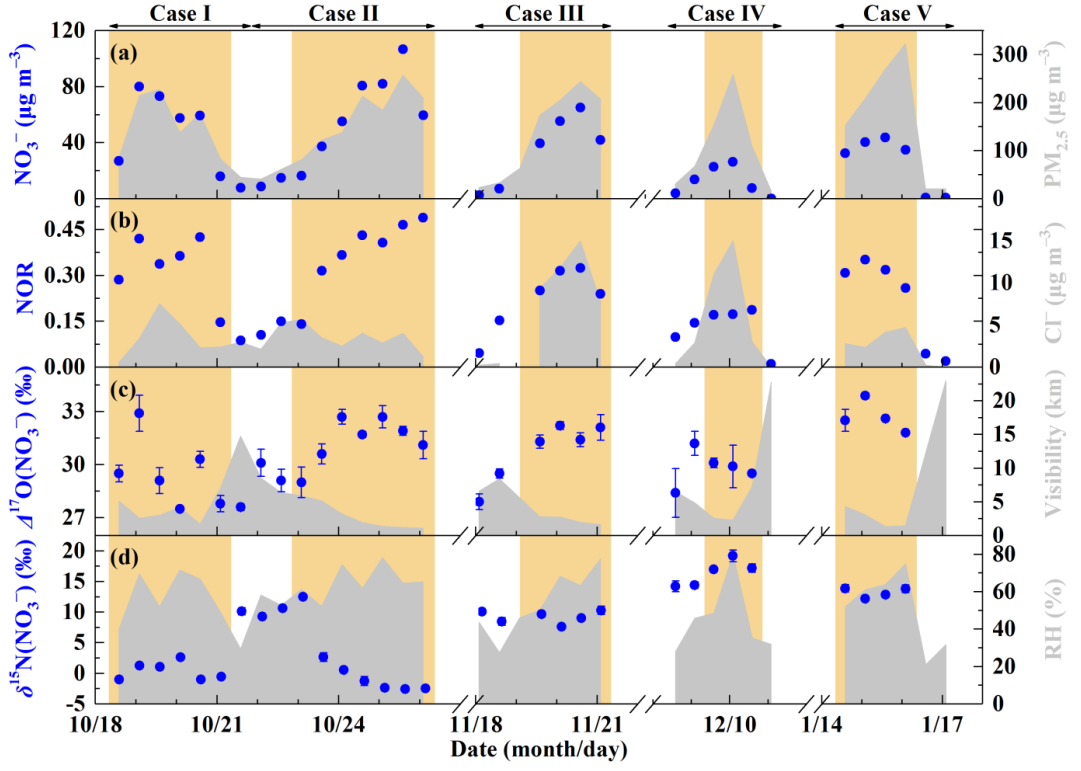

Figure 3. General characteristics of haze events in Beijing (October 2014 – January 2015). **(a)** Time series of $PM_{2.5}$ and NO_3^- concentrations. **(b)** Time series of nitrogen oxidation ratio (NOR, which equals to NO_3^- molar concentration divided by the sum of NO_3^- and NO_2 molar concentration) and Cl^- concentrations. **(c)** Time series of $\Delta^{17}O(NO_3^-)$ and visibility. **(d)** Time series of $\delta^{15}N(NO_3^-)$ and relative humidity (RH). The error bars in (c) and (d) are ±1σ of replicate measurements (n = 3) of each sample. The khaki shaded area indicates polluted days (PD, $PM_{2.5} \geq 75$ μg m^{-3}).

Atmos. Chem. Phys. Discuss., https://doi.org/10.5194/acp-2018-334
Manuscript under review for journal Atmos. Chem. Phys.
Discussion started: 14 May 2018

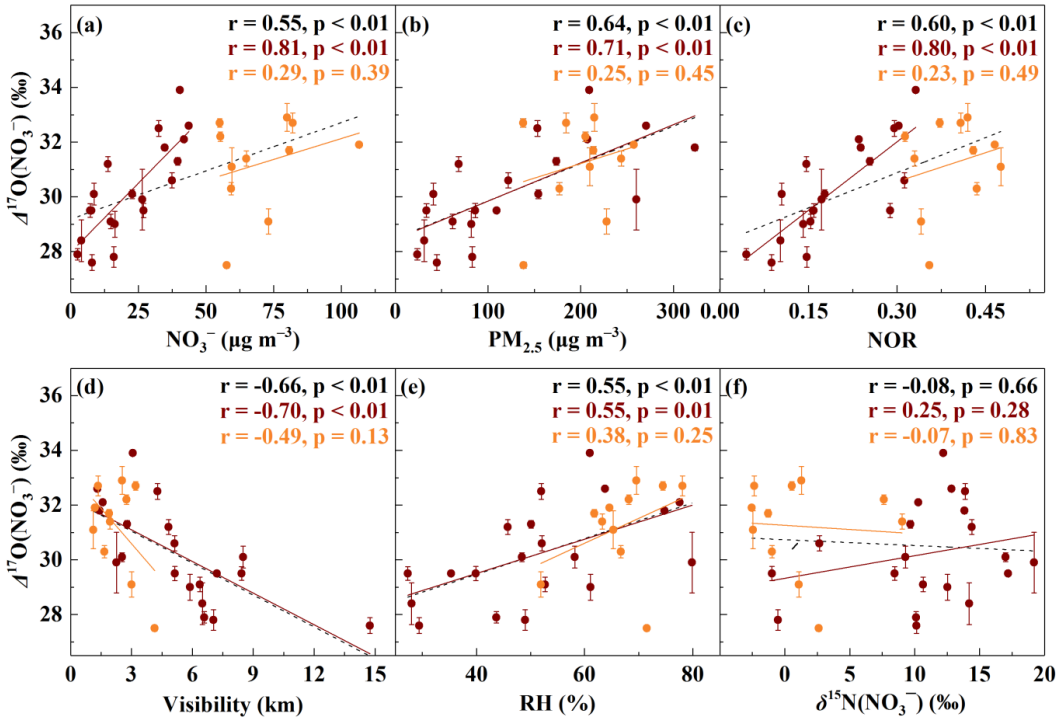

Figure 4. Relationships between $\Delta^{17}O(NO_3^-)$ and other parameters. The relationship between $\Delta^{17}O(NO_3^-)$ and NO_3^- concentrations (**a**), $PM_{2.5}$ concentrations (**b**), nitrogen oxidation ratio (NOR, **c**), visibility (**d**), relative humidity (RH, **e**) and $\delta^{15}N(NO_3^-)$ (**f**). The wine dots are samples with NO_3^- < 50 μg m^{-3} and the orange dots are samples with NO_3^- > 50 μg m^{-3}. The black dash lines are linear least-squares fitting lines for all samples, the wine solid lines are linear least-squares fitting lines for samples with NO_3^- < 50 μg m^{-3} and the orange solid lines are linear least-squares fitting lines for samples with NO_3^- > 50 μg m^{-3}. The error bars are ±1σ of replicate measurements of each sample.

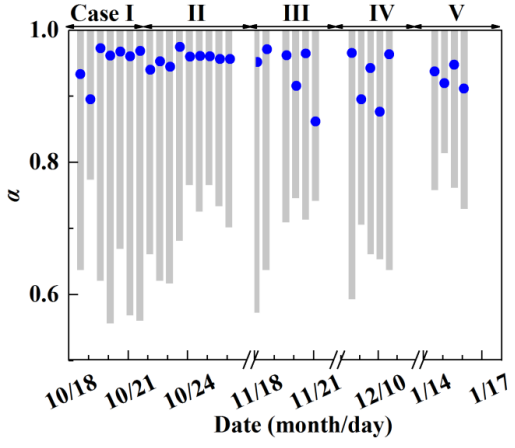

Figure 5. Estimate of the proportion of O_3 oxidation in NO_X cycling, α. The gray column represents possible α range

Atmos. Chem. Phys. Discuss., https://doi.org/10.5194/acp-2018-334
Manuscript under review for journal Atmos. Chem. Phys.
Discussion started: 14 May 2018

Atmospheric Chemistry and Physics Discussions

535 determined by $\Delta^{17}O(NO_3^-)$. The blue dot represents specific α value calculated by Eq. (3).

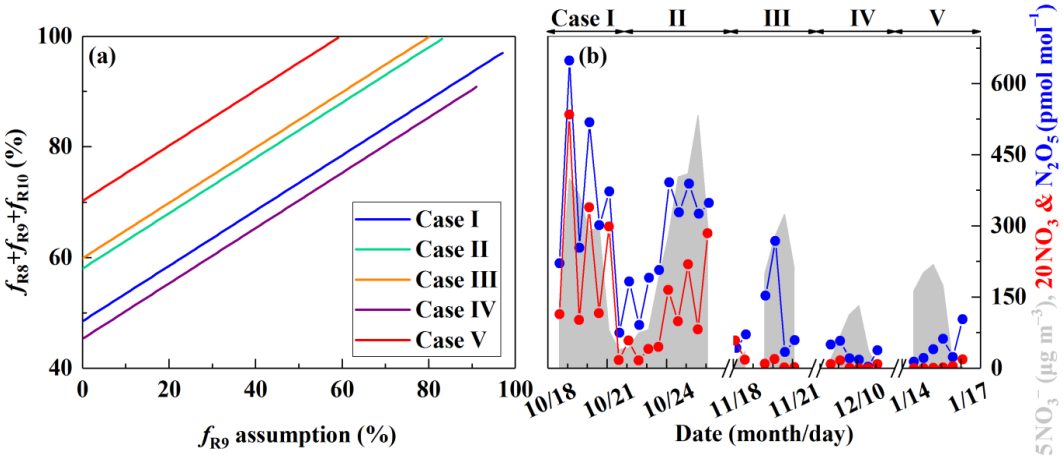

536

537 **Figure 6.** Estimate of the nocturnal formation pathways. The estimated relative importance of nocturnal formation pathways
538 (f_{R8} + f_{R9} + f_{R10}) during PD of each case on the basis of observed $\Delta^{17}O(NO_3^-)$ (See Sect. 2.3, **a**) and the simulated mixing
539 ratios of N_2O_5 and NO_3 radical by MCM (**b**). R8, R9 and R10 in (a) represents NO_3 + HC, N_2O_5 + H_2O and N_2O_5 + Cl^-
540 pathway, respectively.

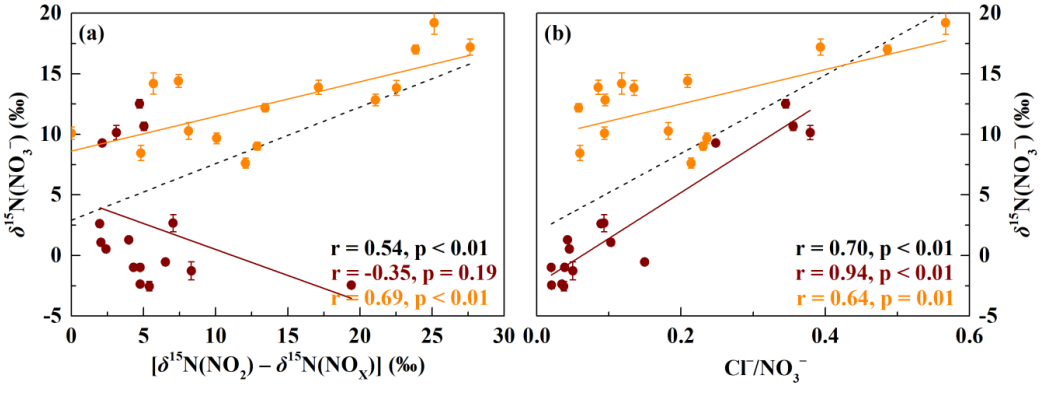

541

542 **Figure 7.** Relationships between $\delta^{15}N(NO_3^-)$ and $[\delta^{15}N(NO_2) - \delta^{15}N(NO_X)]$ **(a)** and mass ratio of Cl^-/ NO_3^- **(b)**. The wine
543 dots are samples in October and the orange dots are samples in residential heating season. The black dash lines are linear
544 least-squares fitting lines for all samples, the wine solid lines are linear least-squares fitting lines for samples in October and
545 the orange solid lines are linear least-squares fitting lines for samples in residential heating season. The error bars are ±1σ of
546 replicate measurements of each sample.

547 **Table 1.** Isotope assumptions of different nitrate formation pathways.

No.	Reaction	$\Delta^{17}O$ of product		Reference
		Expression	Value (‰) [a]	

Atmos. Chem. Phys. Discuss., https://doi.org/10.5194/acp-2018-334
Manuscript under review for journal Atmos. Chem. Phys.
Discussion started: 14 May 2018

Atmospheric Chemistry and Physics Discussions

R1	$NO + O_3 \rightarrow NO_2 + O_2$	$\Delta^{17}O(NO_2) = 1.18 \times \Delta^{17}O(O_3) + 6.6$ ‰	37.28	(Savarino et al., 2008)
R2	$NO + HO_2/RO_2 \rightarrow NO_2 + OH/RO$	$\Delta^{17}O(NO_2) = 0.0$	0.0	(Sofen et al., 2014)
R4	$NO_2 + O_3 \rightarrow NO_3 + O_2$	$\Delta^{17}O(NO_3) = \frac{2}{3}\Delta^{17}O(NO_2) + \frac{1}{3}(1.23 \times \Delta^{17}O(O_3) + 9.0$ ‰)	24.85α + 13.66	(Berhanu et al., 2012)
R5	$NO_2 + NO_3 \rightarrow N_2O_5$	$\Delta^{17}O(N_2O_5) = \frac{2}{5}\Delta^{17}O(NO_2) + \frac{3}{5}\Delta^{17}O(NO_3)$	29.82α + 8.20	(Sofen et al., 2014)
R6	$NO_2 + OH \rightarrow HNO_3$	$\Delta^{17}O(NO_3^-) = \frac{2}{3}\Delta^{17}O(NO_2)$	24.85α	(Sofen et al., 2014)
R7	$2NO_2 + H_2O \rightarrow HNO_3 + HNO_2$	$\Delta^{17}O(NO_3^-) = \frac{2}{3}\Delta^{17}O(NO_2)$	24.85α	[b]
R8	$NO_3 + HC \rightarrow HNO_3 + products$	$\Delta^{17}O(NO_3^-) = \Delta^{17}O(NO_3)$	24.85α + 13.66	(Sofen et al., 2014)
R9	$N_2O_5 + H_2O \rightarrow 2HNO_3$	$\Delta^{17}O(NO_3^-) = \frac{5}{6}\Delta^{17}O(N_2O_5)$	24.85α + 6.83	(Sofen et al., 2014)
R10	$N_2O_5 + Cl^- \rightarrow HNO_3 + ClNO_2$	$\Delta^{17}O(NO_3^-) = \Delta^{17}O(NO_3)$	24.85α + 13.66	[c]

[a] The values are calculated on assumptions that bulk $\Delta^{17}O(O_3)$ = 26 ‰ (Vicars and Savarino, 2014; Ishino et al., 2017) and $\Delta^{17}O(HO_2/RO_2)$ = 0 ‰. $\Delta^{17}O(RO_2)$ is equal to 0 ‰ in the troposphere (Morin et al., 2011), in contrast, observations suggest $\Delta^{17}O(HO_2)$ = 1 – 2 ‰ (Savarino and Thiemens, 1999). However, the difference in calculated $\Delta^{17}O(NO_3^-)$ between assuming $\Delta^{17}O(HO_2)$ = 0 ‰ and $\Delta^{17}O(HO_2)$ = 2 ‰ is negligible in this study (< 0.1 ‰). And the assumption that $\Delta^{17}O(HO_2)$ = 0 ‰ simplifies calculations and is also consistent with previous studies (Michalski et al., 2003; Alexander et al., 2009; Morin et al., 2008; Kunasek et al., 2008; Sofen et al., 2014). α is the proportion of O_3 oxidation in NO_X cycling, calculated by Eq. (3).

[b] Previous studies suggest that in R7 one oxygen atom of NO_3^- is from H_2O and the other two are from NO_2 (Li et al., 2010; Cheung et al., 2000; Goodman et al., 1999), which will result in $\Delta^{17}O(NO_3^-) = 2/3\Delta^{17}O(NO_2)$.

[c] R4 and R5 suggest that the central oxygen atom of N_2O_5 (O_2N-O-NO_2) is from NO_3 radical (O-NO_2) with $\Delta^{17}O$ (‰) = $1.23 \times \Delta^{17}O(O_3)$ + 9.0 ‰. R10 is suggested to occur via O_2N-O-NO_2 (aq) ↔ $NO_2^+ + NO_3^-$ and the following $NO_2^+ + Cl^- \rightarrow ClNO_2$ (Bertram and Thornton, 2009), so $\Delta^{17}O(NO_3^-) = 1/3(1.23 \times \Delta^{17}O(O_3) + 9.0$ ‰) + $2/3\Delta^{17}O(NO_2) = \Delta^{17}O(NO_3)$.

Table 2. Reaction expressions for different NO_2 production pathways.

No.	Reaction	Rate expression	Rate constant (cm^3 $molecule^{-1}$ s^{-1})	Reference
R1	$NO + O_3 \rightarrow NO_2 + O_2$	$k_{R1}[NO][O_3]$	$k_{R1}=3.0 \times 10^{-12} \times e^{(-1500/T)}$	(Burkholder et al., 2015)
R2a	$NO + HO_2 \rightarrow NO_2 + OH$	$k_{2Ra}[NO][HO_2]$	$k_{2Ra}=3.3 \times 10^{-12} \times e^{(270/T)}$	(Burkholder et al., 2015)
R2b	$NO + RO_2 \rightarrow NO_2 + RO$	$k_{2Rb}[NO][RO_2]$	$k_{2Rb} = k_{2Ra}$	(Burkholder et al., 2015; Kunasek et al., 2008)

Table 3. Atmospheric $\Delta^{17}O(NO_3^-)$ in aerosols obtained from the literature and this study.

Sample location	Sample period	Collection	$\Delta^{17}O$ (‰) range	Reference

Atmos. Chem. Phys. Discuss., https://doi.org/10.5194/acp-2018-334
Manuscript under review for journal Atmos. Chem. Phys.
Discussion started: 14 May 2018

		interval		
Huairou, Beijing (40.41 °N, 116.68 °E)	October 2014 – January 2015	12 h	27.5 – 33.9 (30.6 ±1.8)	This study
Trinidad Head, California (41.0 °N, 124.2 °W)	April – May 2002	1 – 4 days	20.1 – 27.5	(Patris et al., 2007)
La Jolla, California (32.7 °N, 117.2 °W)	March 1997 – April 1998	3 days	20 – 30.8	(Michalski et al., 2003)
Mt. Lulin, Taiwan (23.5 °N, 120.9 °E)	January – December 2010	1 day	2.7 – 31.4 (17 ±7)	(Guha et al., 2017)
Cape Verde Island (16.9 °N, 24.9 °W)	July 2007 – May 2008	2 – 3 days	25.5 – 31.3	(Savarino et al., 2013)
Cruise in costal California (32.8 °N – 38.6 °N)	May – June 2010	2 – 22 h	19.0 – 29.2 (24.1 ±2.2)	(Vicars et al., 2013)
Cruise from 65 °S to 79 °N	September – October 2006 April – May 2007 February – April 2006	1 – 4 days	Non-polar: 24 – 33 Polar: 35 ±2	(Morin et al., 2009)
Alert, Nunavut (82.5 °N, 62.3 °W)	March – May 2004	3 – 4 days	29 – 35 (32.7 ±1.8)	(Morin et al., 2007b)
Barrow, Alaska (71.3 °N, 156.9 °W)	March 2005	1 day	26 – 36	(Morin et al., 2007a)
Dumont d'Urville, Antarctic (66.7 °S, 140.0 °E)	January – December 2001	10 – 15 days	20.0 – 43.1	(Savarino et al., 2007)
Dumont d'Urville, Antarctic (66.7 °S, 140.0 °E)	January 2011 – January 2012	7 days	23.0 – 41.9	(Ishino et al., 2017)

Table 4 The possible range of fractional contribution of different nitrate formation pathways during PD of each case estimated on the basis of observed $\Delta^{17}O(NO_3^-)$ [a].

PD of Case	f_{R9} assumption (%)	$f_{R8} + f_{R9} + f_{R10}$ (%)	$f_{R8} + f_{R10}$ (%)	$f_{R6} + f_{R7}$ (%)
I	0 – 97	49 – 97	0 – 49	3 – 51
II	0 – 83	58 – 100	17 – 58	0 – 42
III	0 – 80	60 – 100	20 – 60	0 – 40
IV	0 – 90	45 – 90	0 – 45	10 – 55

Atmos. Chem. Phys. Discuss., https://doi.org/10.5194/acp-2018-334
Manuscript under review for journal Atmos. Chem. Phys.
Discussion started: 14 May 2018

V	0 – 59	70 – 100	41 – 70	0 – 30
Average	0 – 82	56 – 97	16 – 56	3 – 44

563 [a] R6, R7, R8, R9 and R10 is respectively NO_2 + OH, NO_2 + H_2O, NO_3 + HC, N_2O_5 + H_2O and N_2O_5 + Cl^- pathway.